

# Generic Contrast Agents

Our portfolio is growing to serve you better. Now you have a *choice*.



[VIEW CATALOG](#)

# AJNR

This information is current as of May 13, 2025.

## **Diffusion Tensor MR Imaging Tractography of the Pyramidal Tracts Correlates with Clinical Motor Function in Children with Congenital Hemiparesis**

O.A. Glenn, N.A. Ludeman, J.I. Berman, Y.W. Wu, Y. Lu, A.I. Barth, D.B. Vigneron, S.W. Chung, D.M. Ferriero, A.J. Barkovich and R.G. Henry

*AJNR Am J Neuroradiol* 2007, 28 (9) 1796-1802

doi: <https://doi.org/10.3174/ajnr.A0676>

<http://www.ajnr.org/content/28/9/1796>

ORIGINAL  
RESEARCH

O.A. Glenn  
N.A. Ludeman  
J.I. Berman  
Y.W. Wu  
Y. Lu  
A.I. Barth  
D.B. Vigneron  
S.W. Chung  
D.M. Ferriero  
A.J. Barkovich  
R.G. Henry

# Diffusion Tensor MR Imaging Tractography of the Pyramidal Tracts Correlates with Clinical Motor Function in Children with Congenital Hemiparesis

**BACKGROUND AND PURPOSE:** Children with congenital hemiparesis have greater asymmetry in diffusion parameters of the pyramidal tracts compared with control subjects. We hypothesized that the asymmetry correlates with the severity of hemiparesis and that diffusion metrics would be abnormal in the affected tracts and normal in the unaffected tracts.

**MATERIALS AND METHODS:** Fifteen patients with congenital hemiparesis and 17 age-matched control subjects were studied with diffusion tensor MR imaging tractography. Hemipareses were scored as mild, moderate, or severe. We measured tract-specific diffusion parameters (fractional anisotropy, mean, and directional diffusion coefficients) of the pyramidal tracts. We compared tract-specific parameters and asymmetry between the right and left tracts of the differing severity groups and control subjects.

**RESULTS:** We observed many different causes of congenital hemiparesis including venous infarction, arterial infarction, and polymicrogyria. Clinical severity of hemiparesis correlated with asymmetry in fractional anisotropy ( $P < .0001$ ), transverse diffusivity ( $P < .0001$ ), and mean diffusivity ( $P < .03$ ). With increasing severity of hemiparesis, fractional anisotropy decreased ( $P < .0001$ ) and transverse diffusivity ( $P < .0001$ ) and mean diffusivity ( $P < .02$ ) increased in the affected pyramidal tract compared with controls. Diffusion metrics in the unaffected tract were similar to those in the control subjects.

**CONCLUSION:** Asymmetry in fractional anisotropy, transverse diffusivity, and mean diffusivity, as well as the degree of abnormality in the actual values of the affected pyramidal tracts themselves, correlates with the severity of motor dysfunction in infants and children with congenital hemiparesis from different causes. This suggests that abnormalities detected by diffusion tensor MR imaging tractography in the affected pyramidal tract are related to the functional ability of the affected pyramidal tract, regardless of the etiology of motor dysfunction.

Congenital hemiparesis is a common subtype of motor dysfunction, affecting one third of patients with a clinical diagnosis of cerebral palsy.<sup>1</sup> It can result from abnormalities that occur in the prenatal or perinatal period, or both.<sup>1</sup> Although imaging findings are well described, most studies have failed to show a statistically significant correlation between clinical severity of motor dysfunction and MR imaging findings.<sup>2-6</sup> Diffusion tensor MR imaging (DTI) tractography is a noninvasive method to segment specific white matter pathways, such as the pyramidal tracts. Using DTI, the motion of water can be quantified along 3 principal directions, where motion along the direction with the greatest water displacement is represented by the major eigenvalue ( $\lambda_1$ ), and motion along directions perpendicular to the major eigenvalue are represented by the minor eigenvalues ( $\lambda_2$  and  $\lambda_3$ ).<sup>7</sup> By quantifying the motion of water along different directions, DTI provides information about the microstructure and organization of white matter and thus is an excellent method to study disorders of white matter pathways. It is sensitive to microstructural changes,

even in the absence of abnormalities on conventional MR images. The pyramidal tract is especially amenable to study with DTI tractography because of its organization, large size, and the fact that few tracts cross it below the top of the lateral ventricles.

Some preliminary work has shown that DTI is able to discriminate between normal and abnormal pyramidal tracts in children with congenital hemiparesis.<sup>8</sup> To verify this observation, the diffusion characteristics of the pyramidal tracts of 15 children with congenital hemiparesis were measured, analyzed, and compared with those of 17 age-matched control subjects to test the following hypotheses: 1) the asymmetry in diffusion metrics of the pyramidal tracts correlates with the clinical severity of motor dysfunction, and 2) diffusion metrics are abnormal in the affected tracts and normal in the unaffected tracts.

## Materials and Methods

### Patient Population

Fifteen patients with congenital hemiparesis (8 boys, 7 girls) and 17 age-matched controls (7 boys, 10 girls) underwent DTI. Age at MR imaging was adjusted based on gestational age at the time of birth. Our institutional review board approved the study, and informed consent was obtained from the parent(s) or subject (if older than 18 years) after the nature of the procedure had been fully explained. Fourteen patients with congenital hemiparesis underwent DTI as part of a clinical MR imaging to evaluate their hemiparesis, and 1 patient underwent DTI solely for this study.

Control subjects had normal neurodevelopment and motor func-

Received November 18, 2006; accepted after revision February 20, 2007.

From the Departments of Radiology (O.A.G., N.A.L., J.I.B., Y.L., D.B.V., S.W.C., A.J.B., R.G.H.), and Neurology and Pediatrics (Y.W.W., A.I.B., D.M.F., A.J.B.), University of California, San Francisco, San Francisco, Calif.

This study was supported by the Charles A. Dana Clinical Hypotheses Program in Imaging and National Institutes of Health Grant No. M01RR-01271 as well as funding provided in part by a Radiological Society of North America Research Fellowship grant.

Please address correspondence to Orit A. Glenn, UCSF Department of Radiology, Neuro-radiology Section, 505 Parnassus Ave, Box #0628, San Francisco, CA 94143-0628; e-mail: Orit.Glenn@radiology.ucsf.edu

DOI 10.3174/ajnr.A0676

tion and were undergoing clinical MR imaging for the following indications: facial mass ( $n = 4$ ), retinoblastoma ( $n = 2$ ), family history of arteriovenous malformation ( $n = 2$ ), nasal mass ( $n = 1$ ), macrocephaly ( $n = 1$ ), nystagmus ( $n = 1$ ), pineal cyst ( $n = 1$ ), occipital skull lesion ( $n = 1$ ), congenital ventriculomegaly ( $n = 1$ ), headaches ( $n = 1$ ), and a family history of retinoblastoma ( $n = 1$ ). One control subject underwent DTI solely for this study.

### **Clinical Assessment of Hemiparesis**

Hemiparesis was defined as unilateral motor dysfunction associated with at least 1 upper motor neuron sign. All patients had been evaluated clinically by a pediatric neurologist for their hemiparesis. Because all patients were not evaluated by the same pediatric neurologist, a study pediatric neurologist who was blinded to the MR and DTI results reviewed the records of the neurology clinic visit before the MR imaging and assigned a clinical severity score. Patients were defined as having mild congenital hemiparesis if they had mild motor abnormalities in the absence of functional limitations; moderate hemiparesis if motor deficits in the most affected limb were accompanied by functional limitations, including the need of assistive devices such as braces or orthotics; and severe hemiparesis if there was no functional use of the most affected limb.

### **MR Imaging**

We performed DTI on 1.5T MR scanners (GE Signa, LX platform; GE Healthcare, Milwaukee, Wis) by using a single-shot, multi-acquisition echo-planar sequence: TR, 8000 ms; TE, 98 ms; matrix,  $256 \times 128$ ; FOV,  $360 \times 180$  mm; resolution,  $1.4 \times 1.4$  mm in-plane; 3-mm section thickness with no skip; and number of averages, 6. Images were acquired in 14 minutes in the axial plane from approximately 28 section locations with diffusion gradients applied in 6 noncollinear directions with a b-value of  $1000 \text{ s/mm}^2$  and a b-value of zero. All subjects also had 3D SPGR T1-weighted images or 3D FSE T2-weighted images of the entire brain acquired in the coronal plane (1.5 mm, skip 0), as well as axial and sagittal spin-echo T1-weighted images; 14 subjects also had dual-echo spin-echo T2-weighted images acquired in the axial plane (4 mm, skip 2 mm).

### **DTI Processing and Tractography**

DTI images were transferred off-line, and diagonalization of the diffusion tensor<sup>9</sup> was performed with use of our in-house software. Directional diffusivities were defined as parallel diffusivity being the largest eigenvalue, and transverse diffusivity being the average of the minor eigenvalues. We calculated the directionally averaged diffusion or mean diffusivity ( $D_{av}$ ) as the mean of all 3 eigenvalues, and we calculated fractional anisotropy (FA) from the diffusion eigenvalues.<sup>9</sup>

We generated DTI fiber tracks by using an in-house software written in Interactive Data Language (ITT, Boulder, Colo) and based on the published deterministic fiber assignment by continuous tracking algorithm (FACT).<sup>10</sup> The fiber-tracking software can create DTI fiber tracks, visualize the tracks in 3D, and perform quantitative analyses on the delineated tracts. Fiber tracks were launched from starting points in each voxel in the brain. Fiber track trajectories follow the diffusion tensor's primary eigenvector from voxel to voxel in 3D. Tracking of the fiber trajectories was terminated when the fiber tracks made a turn of greater than  $41^\circ$  between 2 successive voxels or if they entered a voxel with fractional anisotropy less than 0.07. We chose this FA threshold value because of lower FA values in the pediatric brain and because of the possibility of reduced FA in the abnormal pyramidal tracts.

To segment the pyramidal tract, we drew 3 filtering regions of interest by using prior anatomic knowledge: the entire caudal cerebral peduncle, posterior two thirds of the posterior limb of the internal capsule at the level of the globus pallidus, and the precentral gyrus in the centrum semiovale. The regions of interest were drawn on the b = 0 echo-planar image because it was unknown to what extent the diffusivity of the tissues was altered in the patients (which would therefore affect our ability to identify the tracts on anisotropy and/or directionally encoded color maps). All regions of interest were drawn by one of the authors (N.A.L.) who remained blinded to the clinical evaluation of the patients, and were always reviewed and approved by a pediatric neuroradiologist (O.A.G.), who was also blinded to the clinical evaluation of the patients. Only fiber tracks passing through all 3 filtering regions of interest were retained as the delineated pyramidal tract. When the precentral gyrus could not be identified, a posterior quadrant region of interest (which encompassed the posterior half of the right or left centrum semiovale) was drawn whenever possible (eg, for the 3 patients with polymicrogyria). Extensive encephalomalacia in 2 patients made it impossible to track rostral to the posterior limb of the internal capsule (because of extremely low anisotropy values); thus, we used the regions of interest of the cerebral peduncle and posterior limb of the internal capsule to generate the tracks on the affected side.

### **Measurement of Tract-Specific Diffusion Metrics**

We made weighted tract-specific measurements (FA, individual eigenvalues, and  $D_{av}$ ) of the pyramidal tract for each side by averaging the measurements in the voxels through which the fiber tracks pass from the cerebral peduncle to the posterior limb of the internal capsule. The contribution of the measurement of a voxel was weighted by the number of fiber-trajectories passing through the voxel. For each patient, asymmetry in weighted tract-specific diffusion measurements between the 2 pyramidal tracts was calculated as the difference in measurements between the 2 sides divided by the measurement of the unaffected side, and was expressed as a percentage. In a similar fashion, we calculated the percentage of asymmetry in weighted tract-specific diffusion measurements for each control subject. The decision of which side to use as the "affected" in the above formula for the control subjects was based on which side was the affected side for their age-matched patients.

### **Statistical Analysis**

We compared asymmetry in the DTI parameters (FA,  $D_{av}$ , transverse, and parallel diffusivities) for the mild, moderate, and severe congenitally hemiparetic group, and the control group by using one-way ANOVA. Those DTI parameters with significant group effect were further analyzed with use of the Student-Newman-Keuls test, correcting for multiple comparisons. To compare diffusion parameters in the affected and unaffected pyramidal tracts of the patients with the control subjects, we used random effects modeling and generated normative linear curves of the natural logarithm of diffusion parameters as a function of age for the controls. We calculated Z-scores for the patients according to their deviation (in root-mean-squared errors of the mean) from the normative control curve. We performed statistical analyses using SAS 9.0 (SAS Institute, Cary, NC) and JMP 5.1 (SAS Institute) using a statistical significance level of 0.05.

## **Results**

### **Clinical Results**

Five patients had mild hemiparesis, 8 had moderate hemiparesis, and 2 patients had severe hemiparesis. Median age was 24.6 months among the patients and 20.2 months in the con-

**Table 1: Characteristics and imaging findings of children with congenital hemiparesis**

Case	Gender	GA at Birth (wks)	Age at MR Imaging (mos)	Severity of Hemiparesis	Hemiparetic side	Conventional MR Imaging Results
1	Male	Term	7.32	Mild	Right	Normal
2	Female	Term	10.84	Mild	Left	Normal
3	Male	27	20.46	Mild	Right	Normal
4	Female	Term	97.23	Mild	Right	Focal volume loss in left posterior frontal PVWM and caudate body with mild ex vacuo dilation of lateral ventricle consistent with venous infarct
5	Female	Term	125.6	Mild	Left	Focal T2 hyperintensity right posterior frontal PVWM with mild ex vacuo dilation of lateral ventricle consistent with venous infarct
6	Female	36	13.63	Moderate	Right	Small focal dilation of right frontal horn in region of caudate head
7	Male	Term	14.58	Moderate	Left	Volume loss in right posterior frontal PVWM with evidence of prior hemorrhage and small right thalamus, consistent with venous infarct
8	Female	37	17.25	Moderate	Left	Right parietotemporal encephalomalacia consistent with MCA angular branch infarct; small right thalamus; small right CP
9	Female	Term	24.55	Moderate	Left	Right frontoparietotemporal polymicrogyria; small right thalamus; small right CP
10	Female	37	32.17	Moderate	Left	Punctate T2 hyperintensity in right parietal PVWM; thin posterior body & splenium of corpus callosum
11	Male	Term	43.16	Moderate	Right	Left frontoparietal polymicrogyria; small left thalamus; small left CP
12	Male	Term	91.55	Moderate	Right	Encephalomalacia left paramedian frontal & parietal lobes with ex vacuo dilation of lateral ventricle consistent with ACA infarct; thin body & splenium of corpus callosum; small left CP
13	Male	Term	209.27	Moderate	Left	Right frontoparietal polymicrogyria; small right CP
14	Male	Term	6.49	Severe	Left	Right frontoparietotemporal cystic encephalomalacia with ex vacuo dilation of lateral ventricle consistent with MCA infarct; small right deep gray nuclei; small right CP
15	Male	37	59.98	Severe	Left	Right frontoparietotemporal cystic encephalomalacia with ex vacuo dilation of lateral ventricle consistent with MCA infarct; small right deep gray nuclei; small right CP

**Note:**—GA indicates gestational age; PVWM, periventricular white matter; CP, cerebral peduncle; MCA, middle cerebral artery; ACA, anterior cerebral artery.

trol subjects. Marked variability in lesions was seen on conventional MR imaging (Table 1). Abnormalities along the course of the pyramidal tract were seen in 2 of 5 patients with mild hemiparesis, 6 of 8 patients with moderate hemiparesis, and in both patients who had severe hemiparesis. Three patients with mild hemiparesis had a normal MR imaging. Three of the patients with moderate hemiparesis had unilateral polymicrogyria involving the frontal and parietal lobes. One patient with moderate hemiparesis had essentially normal MR imaging with only a small focal dilation of the frontal horn in the region of the caudate head ipsilateral to the side of the clinical hemiparesis, and not involving the course of the pyramidal tract. The patients with severe hemiparesis had evidence of unilateral perinatal arterial infarction with cystic encephalomalacia of nearly the entire middle cerebral artery territory. MR imaging findings in the control subjects included a choroidal fissure cyst, a pineal cyst, nonspecific small frontal periventricular white matter T2 hyperintensity, ventriculomegaly, an incidental 1-cm cerebellar vermian juvenile pilocytic astrocytoma, and developmental venous anomalies. No control subjects had any abnormalities along or adjacent to the expected course of the pyramidal tracts.

### DTI Tractography Results

The percentage of asymmetry in FA differed among the 4 groups ( $P < .0001$ ) (Table 2). There was increasing FA asymmetry with increasing severity of congenital hemiparesis (Fig 1). The patients with severe hemiparesis had the greatest asymmetry in FA compared with those who had moderate hemiparesis ( $-47\%$  vs  $-18\%$ ,  $P < .0001$ ), mild hemiparesis ( $-47\%$  vs  $-3\%$ ,  $P < .0001$ ), and the control subjects ( $-47\%$  vs  $-0.3\%$ ,  $P < .0001$ ). The percentage of asymmetry in FA was greater in the patients with moderate hemiparesis compared with the mild hemiparesis group ( $-18\%$  vs  $-3\%$ ,  $P < .0001$ ) and the control subjects ( $-18\%$  vs  $0.3\%$ ,  $P < .0001$ ). Mean asymmetry in FA did not differ in the mild hemiparesis group compared with the control subjects ( $P = .39$ ).

There was a progressive decrease in FA values in the pyramidal tracts contralateral to the hemiparesis (ie, affected side) with increasing severity of hemiparesis ( $P < .0001$ ). Compared with the control subjects, FA was lower in the affected tracts in the patients with severe hemiparesis ( $P < .0001$ ) as well as in the patients with moderate hemiparesis ( $P = .0002$ ) (Fig 2A). The patients with mild hemiparesis did not have significantly lower values of FA in the affected pyramidal tracts

**Table 2: Comparison of mean percent asymmetry of diffusion parameters\***

Subject Category	Fractional Anisotropy	Transverse Diffusivity	Parallel Diffusivity	D <sub>av</sub>
Control	0.3% (3.8, -3.2)	-1.3% (4.9, -7.5)	-0.5% (2.6, -3.7)	-1.9% (6.5, -10.3)
Mild hemiparesis	-2.8% (3.6, -9.3)	3.6% (15.1, -7.9)	-0.9% (4.8, -6.7)	1.6% (17.1, -14.0)
Moderate hemiparesis	-17.7% (-12.6, -22.8)	21.5% (30.6, 12.4)	-3.3% (1.2, -7.9)	6.6% (18.8, -5.7)
Severe hemiparesis	-46.9% (-36.7, -57.1)	75.2% (93.4, 57.1)	7.2% (16.3, -2.0)	38.8% (63.4, 14.2)
P value	$P < .0001†‡$	$P < .0001†‡$	$P = .23†$	$P < .03†‡$

\* 95% confidence intervals are listed in parentheses.

† P values are listed for one-way ANOVA analyses.

‡ P values < .05.

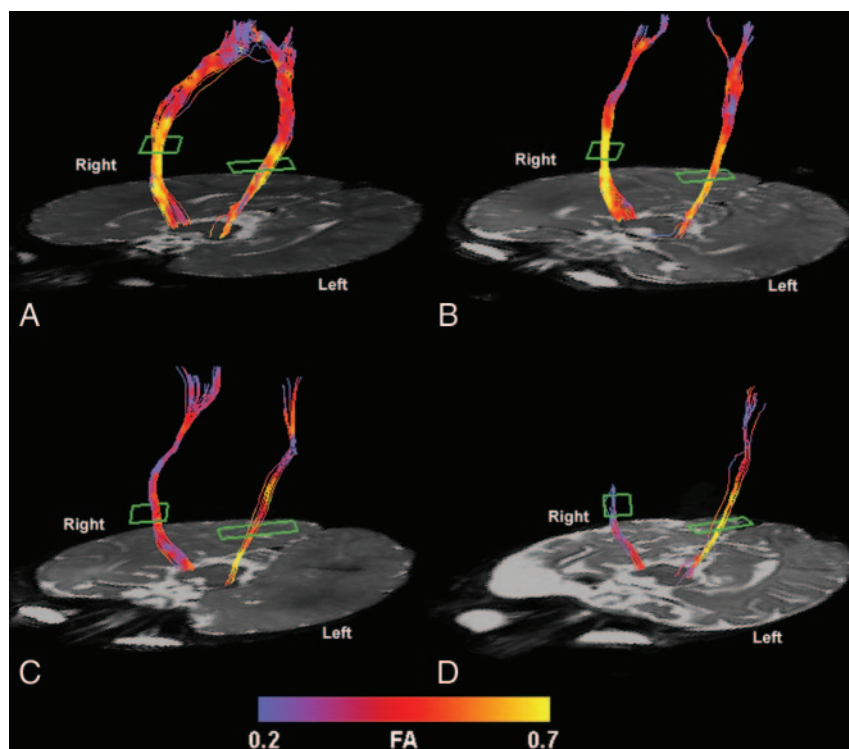


**Fig 1.** Color-coded representation of fractional anisotropy in the pyramidal tracts of a control subject (A), a patient with mild left hemiparesis (B), a patient with moderate left hemiparesis (C), and a patient with severe left hemiparesis (D). Lower fractional anisotropy values are seen in the affected pyramidal tract compared with the unaffected tract of the patients with moderate and severe hemiparesis. The patient with mild hemiparesis and the control subject show no appreciable asymmetry. Although the entire tract is shown from the level of the cerebral peduncle to the centrum semiovale, the analysis was limited to that portion of the pyramidal tract between the posterior limb of the internal capsule (outlined in green) and the cerebral peduncle (see Methods).

compared with the control subjects. FA in the affected tracts was also lower than FA in the unaffected tracts ( $P = .003$ ) in the patients. FA in the unaffected pyramidal tracts of the patients was similar to that in the control subjects.

The percentage of asymmetry in transverse diffusivity also differed among the 4 groups ( $P < .0001$ ) (Table 2). Asymmetry in transverse diffusivity increased with increasing severity of congenital hemiparesis. Asymmetry in transverse diffusivity was highest in those children with severe hemiparesis compared with those with moderate hemiparesis (75% vs 22%,  $P < .0001$ ), mild hemiparesis (75% vs 4%,  $P < .0001$ ), and the control subjects (75% vs -1%,  $P < .0001$ ). The patients with moderate hemiparesis also had greater asymmetry in transverse diffusivity compared with those with mild hemiparesis (22% vs 4%,  $P = .02$ ) and the control subjects (22% vs -1%,  $P < .0002$ ). There was no difference in asymmetry in transverse diffusivity between the patients with mild hemiparesis and the control subjects ( $P = .45$ ).

There was a progressive increase in transverse diffusivity of the affected pyramidal tracts with increasing severity of hemiparesis ( $P < .0001$ ). Compared with the control subjects, transverse diffusivity was greater in the affected pyramidal tract of the patients with severe hemiparesis ( $P < .0001$ ) and in the affected pyramidal tract of the patients with moderate

hemiparesis ( $P = .002$ ) (Fig 2B). The patients with mild hemiparesis had similar transverse diffusivity values compared with the control subjects. Transverse diffusivity was also greater in the affected pyramidal tract compared with the unaffected pyramidal tract in the patients ( $P = .006$ ). There was no significant difference in transverse diffusivity of the unaffected pyramidal tracts in the patients compared with the control subjects.

The percentage of asymmetry in D<sub>av</sub> differed among the 4 groups ( $P < .03$ ). There was an increase in D<sub>av</sub> asymmetry with increasing severity of congenital hemiparesis (Table 2). The patients with severe hemiparesis had greater asymmetry compared with those who had moderate hemiparesis (39% vs 7%,  $P = .02$ ) or mild hemiparesis (39% vs 2%,  $P = .01$ ), and the control subjects (39% vs -2%,  $P = .003$ ). There was a trend toward greater asymmetry in D<sub>av</sub> in the moderate hemiparesis group compared with both the mild hemiparesis group and the control subjects, though this did not reach statistical significance.

There was a progressive increase in D<sub>av</sub> values of the affected pyramidal tracts with increasing severity of hemiparesis compared with the control subjects ( $P < .02$ ). D<sub>av</sub> was greater in the affected pyramidal tract of the patients with severe hemiparesis compared with the control subjects ( $P < .02$ ) (Fig



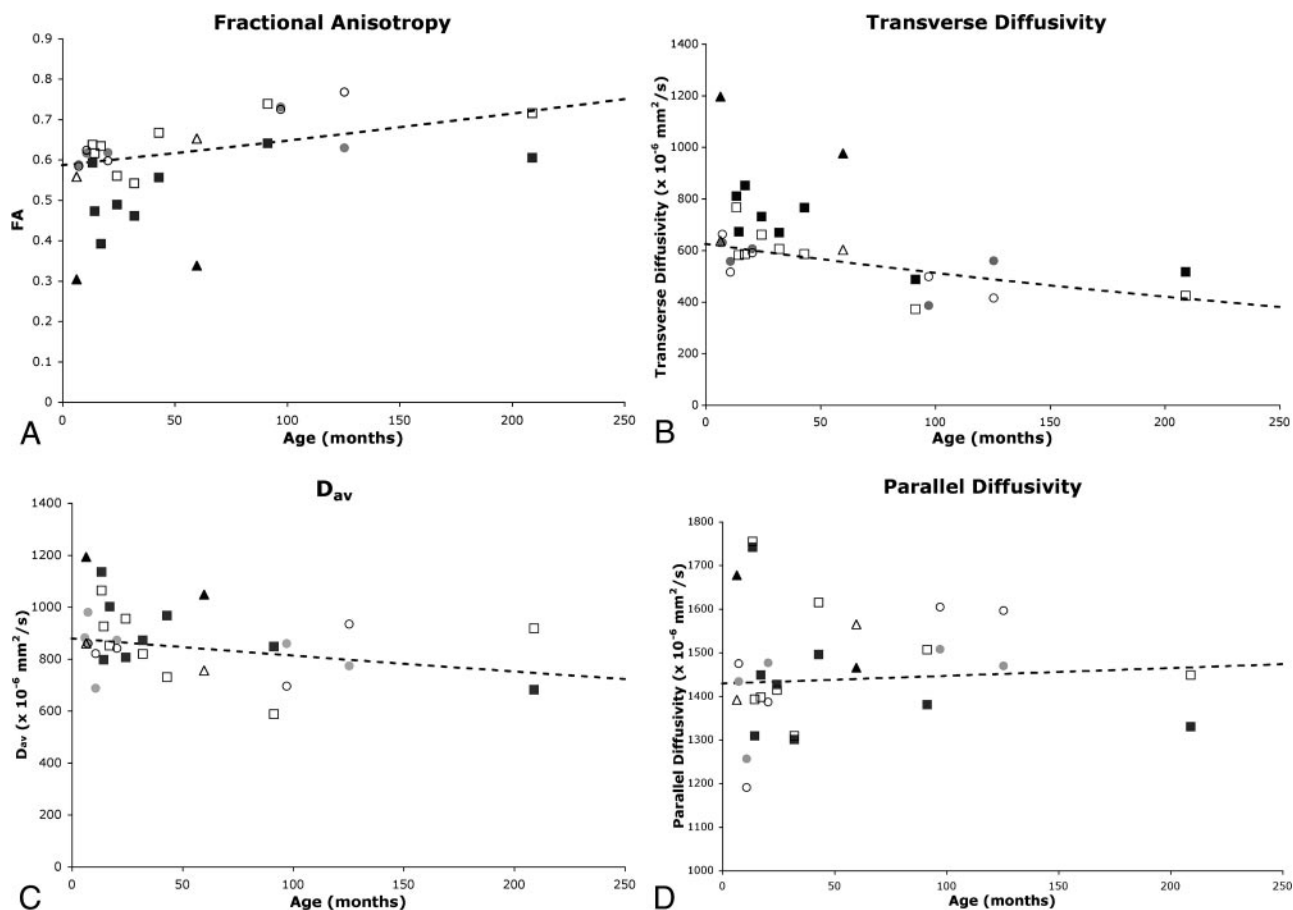


**Fig 2.** Comparison of diffusion parameters in affected and unaffected tracts of the patients with normative curves. Fractional anisotropy (A), transverse diffusivity (B),  $D_{av}$  (C), and parallel diffusivity (D) are plotted against age for the patients with mild hemiparesis (circles), those with moderate hemiparesis (squares), and those with severe hemiparesis (triangles). Both affected (solid symbol) and unaffected (open symbol) pyramidal tract diffusion values are plotted for each patient. Values are compared with the normative curves (dashed curve) of the natural logarithm of the diffusion metric versus age (see Methods).

2C). There was a trend toward increased  $D_{av}$  in the affected tracts of children with moderate hemiparesis compared with the control subjects, but this did not reach statistical significance. The patients with mild hemiparesis did not have significantly greater values of  $D_{av}$  in the affected pyramidal tracts compared with the control subjects.  $D_{av}$  values in the unaffected pyramidal tracts of the patients were not statistically different from those of the control subjects.

The percentage of asymmetry in parallel diffusivity did not differ among the 4 groups (Table 2). There was no significant correlation of parallel diffusivity in the affected tracts with severity of hemiparesis (Fig 2D). There was no correlation of asymmetry in diffusion properties with age in either the patients or control subjects, except for asymmetry in parallel diffusivity, which decreased with increasing age. There were no significant differences between the left and right sides of the control subjects for FA, transverse diffusivity,  $D_{av}$ , or parallel diffusivity.

## Discussion

We observed a wide range of findings on conventional MR imaging in our patients. These findings are similar to other studies that show that the cause of congenital hemiparesis is heterogeneous.<sup>3-5,11,12</sup> In particular, we observed different causes of hemiparesis within a severity group, as well as an

overlap of causes between different groups. These included arterial infarcts in patients with moderate and severe hemiparesis, venous infarcts in patients with moderate and mild hemiparesis, and absence of any obvious cause in patients with moderate and mild hemiparesis. It is interesting to note that one third of our patients with moderate hemiparesis had unilateral polymicrogyria, which seems to be a common prenatal cause of congenital hemiparesis.<sup>13</sup>

Despite the various causes of hemiparesis in our study (including some patients with no obvious cause for their hemiparesis), we were able to demonstrate a strong correlation of DTI metrics with the clinical severity of motor dysfunction. This is exciting because previous studies that correlate imaging findings with clinical hemiparesis are primarily limited to children with arterial infarcts as the cause of their hemiparesis, many of whom were diagnosed during the perinatal period.<sup>14-17</sup> Our study, however, provides an MR imaging marker that correlates with clinical motor function in infants and children with many different causes of their congenital hemiparesis. Moreover, with the exception of 1 patient, our patients were not diagnosed with a brain abnormality or ischemia during the perinatal period, and thus the cause of their hemiparesis was not known at the time of their clinical presentation and MR imaging. The observation that DTI correlates with motor function is important clinically because it suggests that DTI

can be used as an additional assessment of motor function. This tool would be helpful to clinicians when evaluating infants and young children, who can be particularly difficult to examine in a clinical setting. In those cases, DTI could be performed as part of the clinical MR imaging evaluation of their hemiparesis, as in our study.

The ability of DTI to detect group differences in our heterogeneous patient population indicates that the microstructure within the pyramidal tracts differs between groups regardless of the cause of the congenital hemiparesis. Moreover, our observation of abnormal diffusion metrics in the affected pyramidal tract and normal diffusion metrics in the unaffected pyramidal tract suggests that the severity of motor dysfunction is related to alterations in the microstructure of the affected pyramidal tract. In particular, the water protons in the affected pyramidal tract are characterized by an increase in water diffusion perpendicular to the tracts, resulting in a decrease in anisotropy. The increased transverse diffusivity and unchanged parallel diffusivity have been previously associated with wallerian degeneration in arterial infarcts<sup>16,18</sup> and is thought to reflect pathologic changes that involve loss of myelin, axonal loss, myelin debris, and inflammatory edema.<sup>19</sup> However, our patient population includes patients without arterial infarcts. Thus, other mechanisms must also result in the observed diffusion pattern. Moreover, it appears that the pattern on DTI, rather than the mechanism responsible for the changes, is what correlates with clinical function.

A correlation between motor function and diffusion properties has been observed in adults with multiple sclerosis<sup>20</sup> and amyotrophic lateral sclerosis.<sup>21–23</sup> These results have been attributed to damage in the structure of the affected axons and their surrounding myelin sheaths or the effects of the invasion of inflammatory cells, or both. However, studies in children with motor dysfunction are limited, and the mechanisms causing the hemiparesis are quite different as well, so it was of interest to investigate whether similar findings would be discovered as in adult disorders.

A previous study on children with congenital hemiparesis demonstrated a trend toward increasing asymmetry in FA and transverse diffusivity with increasing severity of motor dysfunction, though the study was limited to 4 patients with mild and moderate hemiparesis.<sup>8</sup> Our study extends the previously reported work to a larger group of children with varying severity, as well as varying causes, of hemiparesis and demonstrates statistically significant correlation of DTI metrics with clinical severity of motor dysfunction when compared with normal children. This study also establishes that, in addition to asymmetry, the actual FA and transverse diffusivity metrics are abnormal in the affected tracts and normal in the unaffected tracts. Furthermore, the degree of abnormality in the affected tracts correlates with the severity of hemiparesis. This finding provides a future framework for analyzing such effects in subjects with bilateral motor abnormalities of varying degrees of severity.

Our study supports the observation of Wiesmann et al<sup>24</sup> that FA was more severely reduced in 3 adults with severe hemiparesis (some with perinatal origin) compared with adult control subjects. Our results are also in agreement with a study by Khong et al,<sup>16</sup> in which they studied children with hemiparesis caused by middle cerebral arterial infarcts and demon-

strated a correlation between FA asymmetry and motor function, which was attributed to wallerian degeneration along the corticospinal tracts. Our study extends these observations to a larger group of children with many different causes of their hemiparesis, including malformations of cortical development, and some who had hemiparesis with no obvious cause. Moreover, our study also demonstrates a correlation of FA in the affected tracts with the severity of hemiparesis and further investigates the role of directional diffusivities. By demonstrating a correlation of increased transverse diffusivity in the affected tracts with increasing severity of hemiparesis, our findings provide further insight into the microstructural alterations of the affected tracts. In addition, our observations apply to a younger group of children, including infants, when they are more likely to present clinically with signs of hemiparesis. Indeed, DTI tractography may prove helpful in the prediction of long-term outcome in infants with motor dysfunction. In addition, DTI tractography may also be helpful in studying other pediatric disorders, such as those involving the visual system, which may also have many different causes and outcomes. Future studies are needed to test these hypotheses.

Although the amount of diffusion asymmetry correlated with the severity of congenital hemiparesis, we did not observe a statistically significant difference between the patients with mild hemiparesis and the control subjects. It is possible that the difference between the children with mild hemiparesis and the control subjects is too small to be detected by our sample size, or that our technique was not adequately sensitive to detect the changes. Further studies with higher signal-to-noise ratio (ie, at higher field strength or with parallel imaging) or with a larger group of patients would be necessary to determine whether more subtle abnormalities can be detected.

Another limitation of our study was that we only analyzed the pyramidal tract from the cerebral peduncle to the posterior limb of the internal capsule. This decision was made because errors in DTI tractography result from the difficulty in resolving crossing fibers within a single voxel, which is more likely to occur above the level of the posterior limb of the internal capsule. Thus, by limiting our analysis to the most compact portion of the pyramidal tract, we minimized potential contributions from other tracts. Studies with high angular resolution diffusion imaging (HARDI) are currently under way in an attempt to analyze the entirety of the pyramidal tracts in the cerebrum.

## Conclusion

In summary, we observed a significant correlation between the severity of motor dysfunction and the degree of asymmetry in diffusion metrics (FA, transverse diffusivity, and  $D_{av}$ ) in infants and children with congenital hemiparesis of many different causes. There was a significant progressive decrease in FA and a progressive increase in transverse diffusivity and  $D_{av}$  in the affected pyramidal tracts with increasing clinical severity of hemiparesis, whereas the unaffected tracts exhibited normal diffusion metrics. Future studies will determine whether early measurements of these parameters may be indicative of potential outcome and whether this technique is equally applicable to other systems within the central nervous system.

## References

- Hagberg B, Hagberg G, Beckung E, et al. Changing panorama of cerebral palsy in Sweden. VIII. Prevalence and origin in the birth year period 1991–94. *Acta Paediatr* 2001;90:271–77
- Cioni G, Bartalena L, Biagioni E, et al. Neuroimaging and functional outcome of neonatal leukomalacia. *Behav Brain Res* 1992;49:7–19
- Humphreys P, Whiting S, Pham B. Hemiparetic cerebral palsy: clinical pattern and imaging in prediction of outcome. *Can J Neurol Sci* 2000;27:210–19
- Kotlarek F, Rodewig R, Brull D, et al. Computed tomographic findings in congenital hemiparesis in childhood and their relation to etiology and prognosis. *Neuropediatrics* 1981;12:101–09
- Molteni B, Oleari G, Fedrizzi E, et al. Relation between CT patterns, clinical findings and etiological factors in children born at term, affected by congenital hemiparesis. *Neuropediatrics* 1987;18:75–80
- Wiklund LM, Uvebrant P. Hemiplegic cerebral palsy: correlation between CT morphology and clinical findings. *Dev Med Child Neurol* 1991;33:512–23
- Basser PJ, Pierpaoli C. A simplified method to measure the diffusion tensor from seven MR images. *Magn Reson Med* 1998;39:928–34
- Glenn O, Henry R, Berman J, et al. DTI-based three-dimensional tractography detects differences in the pyramidal tracts of infants and children with congenital hemiparesis. *J Magn Reson Imaging* 2003;18:641–48
- Basser PJ, Pierpaoli C. Microstructural and physiological features of tissues elucidated by quantitative-diffusion-tensor MRI. *J Magn Reson B* 1996;111:209–19
- Mori S, Crain BJ, Chacko VP, et al. Three-dimensional tracking of axonal projections in the brain by magnetic resonance imaging. *Ann Neurol* 1999;45:265–69
- Takanashi J, Barkovich AJ, Ferriero DM, et al. Widening spectrum of congenital hemiplegia: Periventricular venous infarction in term neonates. *Neurology* 2003;61:531–33
- Wu YW, Lindan CE, Henning LH, et al. Neuroimaging abnormalities in infants with congenital hemiparesis. *Pediatr Neurol* 2006;35:191–96
- Pascual-Castroviejo I, Pascual-Pascual SI, Viano J, et al. Unilateral polymicrogyria: a common cause of hemiplegia of prenatal origin. *Brain Dev* 2001;23:216–22
- Bouza H, Dubowitz LM, Rutherford M, et al. Late magnetic resonance imaging and clinical findings in neonates with unilateral lesions on cranial ultrasound. *Dev Med Child Neurol* 1994;36:951–64
- de Vries LS, van der Grond J, van Haastert IC, et al. Prediction of outcome in new-born infants with arterial ischaemic stroke using diffusion-weighted magnetic resonance imaging. *Neuropediatrics* 2005;36:12–20
- Khong PL, Zhou LJ, Ooi GC, et al. The evaluation of Wallerian degeneration in chronic paediatric middle cerebral artery infarction using diffusion tensor MR imaging. *Cerebrovasc Dis* 2004;18:240–47
- Mazumdar A, Mukherjee P, Miller JH, et al. Diffusion-weighted imaging of acute corticospinal tract injury preceding Wallerian degeneration in the maturing human brain. *AJNR Am J Neuroradiol* 2003;24:1057–66
- Pierpaoli C, Barnett A, Pajevic S, et al. Water diffusion changes in Wallerian degeneration and their dependence on white matter architecture. *Neuroimage* 2001;13:1174–85
- Henry RG, Oh J, Nelson SJ, et al. Directional diffusion in relapsing-remitting multiple sclerosis: a possible in vivo signature of Wallerian degeneration. *J Magn Reson Imaging* 2003;18:420–26
- Wilson M, Tench CR, Morgan PS, et al. Pyramidal tract mapping by diffusion tensor magnetic resonance imaging in multiple sclerosis: improving correlations with disability. *J Neurol Neurosurg Psychiatry* 2003;74:203–07
- Graham JM, Papadakis N, Evans J, et al. Diffusion tensor imaging for the assessment of upper motor neuron integrity in ALS. *Neurology* 2004;63:2111–19
- Hong YH, Lee KW, Sung JJ, et al. Diffusion tensor MRI as a diagnostic tool of upper motor neuron involvement in amyotrophic lateral sclerosis. *J Neurol Sci* 2004;227:73–78
- Sach M, Winkler G, Glauche V, et al. Diffusion tensor MRI of early upper motor neuron involvement in amyotrophic lateral sclerosis. *Brain* 2004;127:340–50
- Wiesmann UC, Clark CA, Symms MR, et al. Anisotropy of water diffusion in corona radiata and cerebral peduncle in patients with hemiparesis. *Neuroimage* 1999;10:225–30